



Original Article

Detection of *TERT* Promoter Mutations Using Targeted Next-Generation Sequencing: Overcoming GC Bias through Trial and Error

Hyunwoo Lee¹, Boram Lee^{2,3}, Deok Geun Kim^{3,4}, Yoon Ah Cho⁵, Jung-Sun Kim^{1,3}, Yeon-Lim Suh¹

¹Department of Pathology and Translational Genomics, Samsung Medical Center, Sungkyunkwan University School of Medicine, Seoul, ²Samsung Genome Institute, Samsung Medical Center, Sungkyunkwan University School of Medicine, Seoul, ³Department of Digital Health, Samsung Advanced Institute of Health Science and Technology, Sungkyunkwan University School of Medicine, Seoul, ⁴Department of Clinical Genomic Center, Samsung Medical Center, Sungkyunkwan University School of Medicine, Seoul, ⁵Department of Pathology, Hallym University Sacred Heart Hospital, Hallym University College of Medicine, Anyang, Korea

Purpose Detection of telomerase reverse transcriptase (*TERT*) promoter mutations is a crucial process in the integrated diagnosis of glioblastomas. However, the *TERT* promoter region is difficult to amplify because of its high guanine-cytosine (GC) content (> 80%). This study aimed to analyze the capturing of *TERT* mutations by targeted next-generation sequencing (NGS) using formalin-fixed paraffin-embedded tissues.

Materials and Methods We compared the detection rate of *TERT* mutations between targeted NGS and Sanger sequencing in 25 cases of isocitrate dehydrogenase (*IDH*)-wildtype glioblastomas and 10 cases of non-neoplastic gastric tissues. Our customized panel consisted of 232 essential glioma-associated genes.

Results Sanger sequencing detected *TERT* mutations in 17 out of 25 glioblastomas, but all *TERT* mutations were missed by targeted NGS. After the manual visualization of the NGS data using an integrative genomics viewer, 16 cases showed a *TERT* mutation with a very low read depth (mean, 21.59; median, 25), which revealed false-negative results using auto-filtering. We optimized our customized panel by extending the length of oligonucleotide baits and increasing the number of baits spanning the coverage of the *TERT* promoter, which did not amplify well due to the high GC content.

Conclusion Our study confirmed that it is crucial to consider the recognition of molecular bias and to carefully interpret NGS data.

Key words Next-generation sequencing, *TERT*, Glioblastoma, GC-rich sequence

Introduction

Telomerase reverse transcriptase (*TERT*) is a catalytic subunit of telomerase [1]. In normal tissues, the activity of telomerase is silenced, but when a single nucleotide variant (SNV) occurs in the two major hotspots [2] of the promoter region, telomerase is activated, which leads to telomere lengthening [3,4]. This series of processes is known to play a critical role in tumorigenesis in solid cancers [1,2,4], including gliomas [5,6].

In the 2016 World Health Organization (WHO) classification of central nervous system tumors, molecular parameters, including the status of the *TERT* promoter, are important for the integrated diagnosis of brain tumors [7]. When astrocytic gliomas harbor one of the following genetic variations: *TERT* promoter mutations, epidermal growth factor receptor (*EGFR*) amplification, or chromosome 7 gain/chromosome 10 loss, even though there is a lack of necrosis or microvascular proliferation, this tumor can be diagnosed as an isocitrate

dehydrogenase (*IDH*)-wildtype glioblastoma, WHO grade IV [8]. Detecting the above molecular alterations in a very limited tumor sample would be the benefit the patients for important prognostic and potentially therapeutic information.

Next-generation sequencing (NGS) is one of the ideal methods for comprehensive molecular profiling of brain tumor. The NGS study can detect molecular alterations in wide genomic regions with relatively fast turnaround time, and low cost. However, the NGS study could yield plentiful information including inaccurate results, the appropriate approaches for extracting accurate information from NGS data would be a crucial step.

The promoter area of *TERT* has a high guanine-cytosine (GC) content (> 80%) and easily forms a secondary structure, such as a hairpin structure [9], resulting in a poor amplification. Therefore, many studies have suggested several ways to more accurately detect mutations in the *TERT* promoter region [10,11]. However, in the case of targeted NGS, which

Correspondence: Yeon-Lim Suh

Department of Pathology and Translational Genomics, Samsung Medical Center, Sungkyunkwan University School of Medicine, 81 Irwon-ro, Gangnam-gu, Seoul 06351, Korea

Tel: 82-2-3410-2761 Fax: 82-2-3410-0025 E-mail: ylsuh76@skku.edu

Received January 22, 2021 Accepted April 30, 2021 Published Online May 3, 2021

targets multiple genes, including *TERT*, the detection of variants in the *TERT* promoter region is often difficult due to poor amplification. In this regard, we planned to compare the results of NGS and Sanger sequencing of *TERT* and sought to find ways to accurately detect variants of the *TERT* promoter region using targeted NGS.

Materials and Methods

1. Case selection

We retrospectively selected 25 cases of *IDH*-wildtype glioblastoma from the NGS data in the pathology file of the Samsung Medical Center. All patients underwent brain tumor surgery. All patients provided informed consent for NGS. All tumors were histologically confirmed as glioblastomas, showing microvascular proliferation (n=25) or necrosis (n=22). Clinical information, such as sex, age, and tumor location, was collected. Tumor location was confirmed using preoperative magnetic resonance imaging. The mean age of the 25 patients was 63.64 years (range, 41 to 83 years; median, 65 years), and the male-to-female ratio was 14:11. The tumors were located in the cerebrum in 22 cases (frontal lobe in 10 cases, temporal in 6, parietal in 3, and frontoparietal in 3) and in the cerebellum in three cases. We also collected 10 anonymized non-neoplastic formalin-fixed paraffin-embedded (FFPE) stomach tissue samples for control.

2. DNA extraction

DNA was extracted from 5- μ m-thick FFPE tissues using a QIAamp DSP DNA FFPE Tissue Kit (Qiagen, Hilden, Germany), and the extracted DNA was quantified using the QUBIT dsDNA BR Assay kit (Thermo Fisher Scientific, Waltham, MA).

3. Library preparation and targeted hybrid capture-based NGS

Target capture was performed according to the manufacturer's protocol using the SureSelect XT automation reagent kit (Agilent, Santa Clara, CA), and a paired-end sequencing library was prepared using a barcode. The size and quality of the genomic DNA were validated using the Genomic DNA Analysis ScreenTape and Genomic DNA Reagent together with the Agilent 4200 Tape station (Agilent). Libraries were sequenced using the TG NextSeq 500/550 High Output Kit v2 (Illumina, Inc., San Diego, CA) and TG NextSeq 500/550 Mid Output Kit v2 (Illumina, Inc.).

4. Panel design and data analysis

We used a targeted sequencing panel pipeline named BrainTumorSCAN for data analysis, which was designed to

cover 232 target genes at the Samsung Genome Institute. The list of 232 target genes is listed in S1 Table.

Paired-end reads were aligned to the human reference genome (GRCh37/hg19) using BWA-MEM v0.7.5 [12], SAMTOOLS v0.1.18 [13], GATK v3.1-1 [14], and Picard v1.93 (<http://broadinstitute.github.io/picard/>). SNVs were detected using MuTect ver. 1.1.4 [15], Lofreq ver. 0.6.1 [16], and VarDict ver. 1.06 [17] software. All of SNVs detected by each software were collected and merged. After collecting and merging, sequencing errors were filtered out through an in-house algorithm [18] and we also excluded variants which had been reported as benign or likely benign in ClinVar (<https://www.ncbi.nlm.nih.gov/clinvar/>). Small insertions and deletions (Indels) < 30 bp in size were detected using Pindel v0.2.5a4 [19]. We used ANNOVAR for annotation of predicted SNVs [18]. Among all variants, genetic alterations with a variant of allele frequency (VAF) lower than 1%, a total read depth (TD) value lower than 50, or a variant read count (VC) value lower than 4 were considered as spurious variants and were excluded. To identify the somatic copy number alterations (CNAs), we calculated the mean read depth of each exon and normalized it according to the depth of the target regions in that sample. This normalized read depth was further standardized by dividing it by the expected read depth of a normal population. The expected read depth at each exon was taken from the median value of the read depth at that exon across a set of normal individual samples. Then, the amplitude of copy numbers was calibrated based on the calculated purity of the tumor cells in the sample for ratiocinating accurate copy numbers. If the calibrated amplitude of the copy number was greater than 4, it was considered as amplification, and if it was lower than 1, it was considered a deletion. Additionally, in case of Log2 scale of the adjusted copy number fold change in chromosomal short or long arm entirely is greater than 1 or lower than -1, it is considered as chromosomal short arm, long arm, or whole chromosomal gain or loss, respectively.

5. Sanger sequencing for *TERT*

Sanger sequencing for the analysis of *TERT* promoter mutation was performed using the following pair of primers as previously reported [20]. Amplification of the genomic DNA was performed using the GeneAmp PCR System 9700 (Applied Biosystems, Foster City, CA) and C1000 Touch Thermal Cycler kit (Bio-Rad, Hercules, CA), according to the manufacturer's instructions. Sanger sequencing was performed using the BigDye Terminator v1.1 Cycle Sequencing Kit (Applied Biosystems). The sequencing reaction was performed both in the forward and reverse direction, and the result was confirmed only when the forward-primer and reverse-primer results were consistent with each other.

Table 1. The result of NGS and Sanger sequencing for TERT promoter area

| Case No. | Surgical diagnosis | WHO grade | NGS TERT promoter (initial) | Sanger sequencing | NGS TERT promoter (after reviewing IGV) | TERT TD | TERT VC | TERT VAF (%) |
|----------|----------------------------|-----------|-----------------------------|--------------------|---|---------|---------|--------------|
| 1 | Glioblastoma, IDH-wildtype | IV | Wild type | Not detected | Wild type | 13 | 0 | 0 |
| 2 | Glioblastoma, IDH-wildtype | IV | Wild type | c.1-146C>T (C250T) | c.1-146C>T (C250T) | 7 | 2 | 28.6 |
| 3 | Glioblastoma, IDH-wildtype | IV | Wild type | c.1-124C>T (C228T) | c.1-124C>T (C228T) | 8 | 6 | 75 |
| 4 | Glioblastoma, IDH-wildtype | IV | Wild type | Not detected | Wild type | 9 | 0 | 0 |
| 5 | Glioblastoma, IDH-wildtype | IV | Wild type | c.1-124C>T (C228T) | c.1-124C>T (C228T) | 16 | 7 | 43.8 |
| 6 | Glioblastoma, IDH-wildtype | IV | Wild type | c.1-124C>T (C228T) | c.1-124C>T (C228T) | 25 | 5 | 20 |
| 7 | Glioblastoma, IDH-wildtype | IV | Wild type | c.1-124C>T (C228T) | Wild type | 2 | 0 | 0 |
| 8 | Glioblastoma, IDH-wildtype | IV | Wild type | c.1-124C>T (C228T) | c.1-124C>T (C228T) | 9 | 2 | 22.2 |
| 9 | Glioblastoma, IDH-wildtype | IV | Wild type | c.1-124C>T (C228T) | c.1-124C>T (C228T) | 14 | 2 | 14.3 |
| 10 | Glioblastoma, IDH-wildtype | IV | Wild type | c.1-146C>T (C250T) | c.1-146C>T (C250T) | 7 | 3 | 42.9 |
| 11 | Glioblastoma, IDH-wildtype | IV | Wild type | Not detected | Wild type | 24 | 0 | 0 |
| 12 | Glioblastoma, IDH-wildtype | IV | Wild type | Not detected | Wild type | 26 | 0 | 0 |
| 13 | Glioblastoma, IDH-wildtype | IV | Wild type | Not detected | Wild type | 25 | 0 | 0 |
| 14 | Glioblastoma, IDH-wildtype | IV | Wild type | c.1-146C>T (C250T) | c.1-146C>T (C250T) | 28 | 6 | 21.4 |
| 15 | Glioblastoma, IDH-wildtype | IV | Wild type | Not detected | Wild type | 17 | 0 | 0 |
| 16 | Glioblastoma, IDH-wildtype | IV | Wild type | c.1-146C>T (C250T) | c.1-146C>T (C250T) | 27 | 13 | 48.2 |
| 17 | Glioblastoma, IDH-wildtype | IV | Wild type | Not detected | Wild type | 28 | 0 | 0 |
| 18 | Glioblastoma, IDH-wildtype | IV | Wild type | c.1-146C>T (C250T) | c.1-146C>T (C250T) | 37 | 10 | 27 |
| 19 | Glioblastoma, IDH-wildtype | IV | Wild type | c.1-146C>T (C250T) | c.1-146C>T (C250T) | 32 | 11 | 34.4 |
| 20 | Glioblastoma, IDH-wildtype | IV | Wild type | c.1-124C>T (C228T) | c.1-124C>T (C228T) | 40 | 6 | 15 |
| 21 | Glioblastoma, IDH-wildtype | IV | Wild type | c.1-124C>T (C228T) | c.1-124C>T (C228T) | 47 | 28 | 59.6 |
| 22 | Glioblastoma, IDH-wildtype | IV | Wild type | c.1-146C>T (C250T) | c.1-146C>T (C250T) | 30 | 6 | 20 |
| 23 | Glioblastoma, IDH-wildtype | IV | Wild type | c.1-124C>T (C228T) | c.1-124C>T (C228T) | 12 | 4 | 33.3 |
| 24 | Glioblastoma, IDH-wildtype | IV | Wild type | c.1-124C>T (C228T) | c.1-124C>T (C228T) | 26 | 11 | 42.3 |
| 25 | Glioblastoma, IDH-wildtype | IV | Wild type | Not detected | Wild type | 28 | 0 | 0 |

IDH, isocitrate dehydrogenase; IGV, integrative genomics viewer; NGS, next-generation sequencing; TD, total read depth; TERT, telomerase reverse transcriptase; VAF, variant allele frequency; VC, variant read count; WHO, World Health Organization.

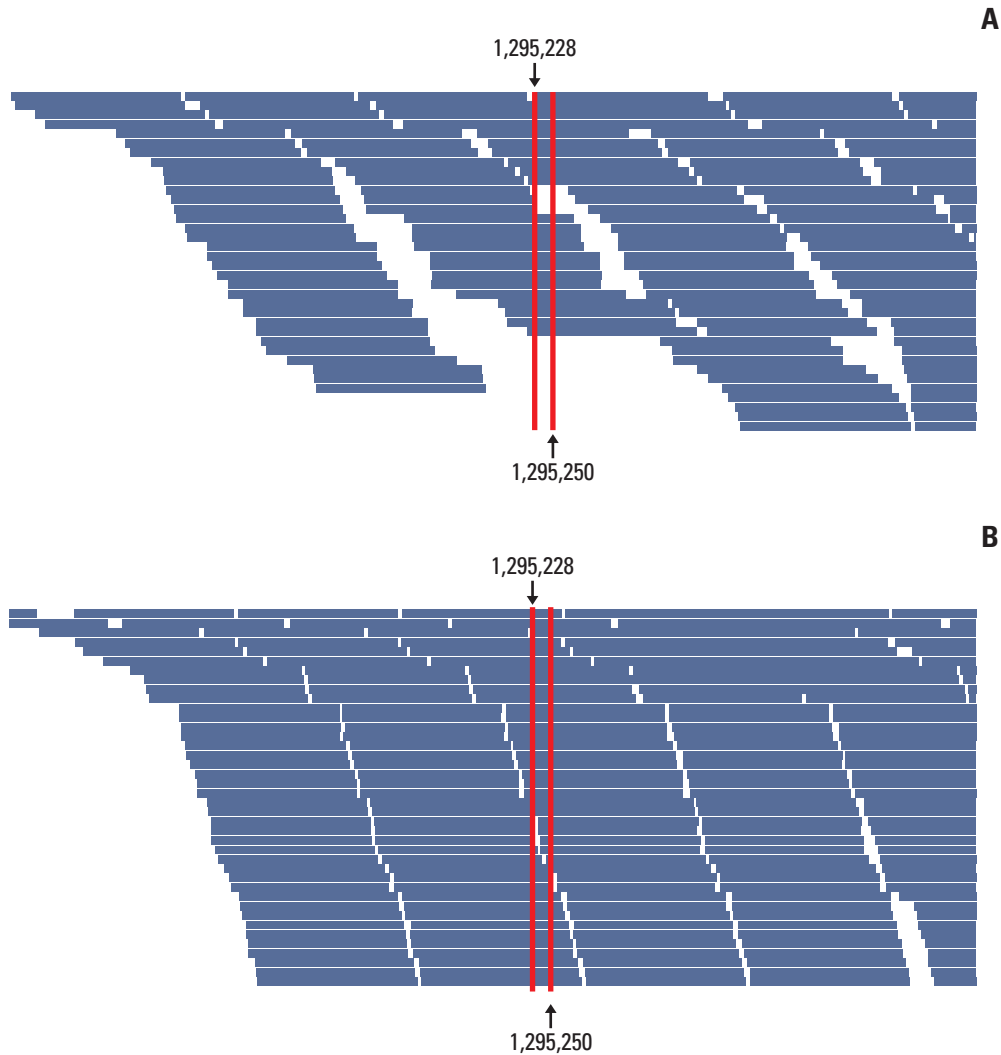


Fig. 3. Optimization of sequence of baits around the telomerase reverse transcriptase (*TERT*) promoter area. After optimization, the number of baits are increased and the length of oligonucleotide sequence of baits are elongated.

sons between non-normally distributed variables, we used Shapiro-Wilk test and Mann-Whitney U test. A p-value lower than 0.05 was considered statistically significant.

Results

1. Detection of *TERT* promoter mutations using targeted NGS and Sanger sequencing

We reviewed the targeted NGS results for 25 glioblastomas. The overall sequencing quality and recommended guideline quality thresholds are summarized in S2 Table adopted from previous study [18]. The average Q30 values of the reads were 92.9% (range, 91.5% to 93.2%) and the on-target rate was 94.2% (range, 93.1% to 95.5%). The ave-

rage TD value was 852.87 ± 91.16 (range, 736.75 to 1,051.0; median, 839.58) and the average rate of uniformity was 78.0% (range, 74% to 81%).

None of the tumors showed any mutations in the *TERT* promoter using targeted NGS, while *TERT* promoter mutations were detected in 17 out of 25 cases (68%) using Sanger sequencing (Table 1). To explore the different detection rates of mutations in the *TERT* promoter using NGS and Sanger sequencing, the aligned reads were manually checked using an integrative genomics viewer (IGV) (<http://software.broadinstitute.org/software/igv/>), considering the possible filtering because of the unsuccessful amplification of the *TERT* promoter. When reviewing the results of the analysis using an IGV (Fig. 1), we found *TERT* mutations in 16 of 25 cases (64%), and their TD, VC, and VAF values are

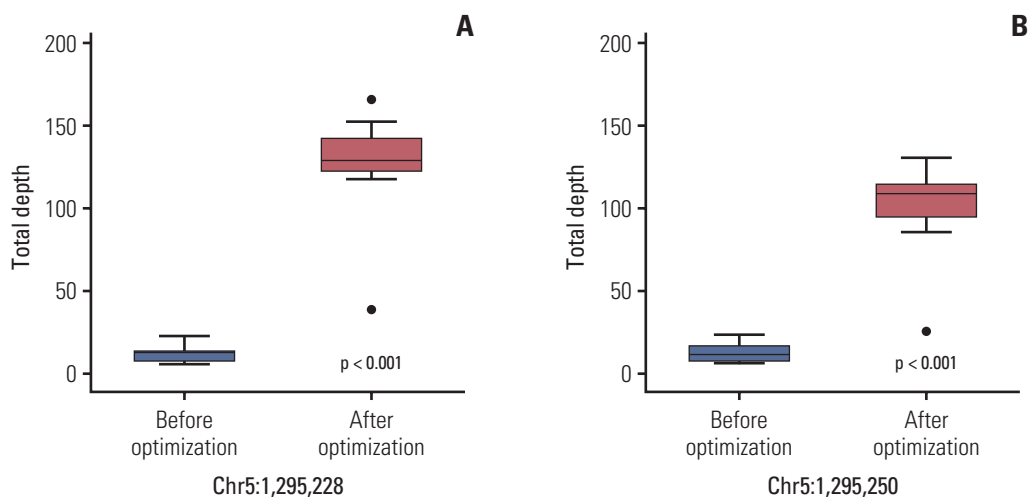


Fig. 4. The mean total read depth of two hotspots (A, Chr 5:1,295,228; B, Chr 5:1,295,250) of telomerase reverse transcriptase (*TERT*) promoter area before and after optimization of baits. After optimization, the mean total read depth of two hotspots are significantly increased (Mann-Whitney U test, $p < 0.001$).

summarized in Table 1. One case (case 7) showed a *TERT* promoter mutation in Chr 5:1,295,228 using Sanger sequencing, but the *TERT* promoter region could not be amplified using targeted NGS. As shown in Table 1, this tumor showed a very low read depth (2) in that position. The average TD value of the *TERT* promoter region was 21.59 (range, 2 to 47; median, 25) and was significantly lower than the average TD values of other genes (mean, 885.40; range, 736.8 to 1,051.0; median, 839.6) ($p < 0.001$) (Fig. 2). The average VC value of the *TERT* promoter mutation was 7.18 ± 6.5 (range, 0 to 28; median, 6), and the average VAF value was 32.2 ± 18.4 (range, 0 to 75; median, 28.6). All cases were excluded for the *TERT* promoter mutation in the original NGS study because of the auto-filtering criteria.

2. Modification of baits design to detect *TERT* mutations

To improve the TD in the *TERT* promoter area, we corrected the design of the capture probe, the so-called baits, which were the single-stranded oligonucleotides used for hybridization with the DNA or RNA in the target capture process. We increased the number of baits around the *TERT* promoter region, especially in two hotspot areas, for increasing the coverage of these baits, and extended the area of the overlapped regions covered by the baits. Then, targeted NGS was performed on 10 cases of non-neoplastic gastric tissues. The results of the analysis of these cases using the IGV showed a change in the distribution of baits around the *TERT* promoter region (Fig. 3). The mean read depth of the two hotspots (Chr 5:1,295,228 and Chr 5:1,295,250) where mutations occur predominantly in the *TERT* promoter region were originally 12.3 and 13.1, respectively. After the modification of the baits

in the *TERT* promoter region, the mean read depth of the two hotspots increased significantly to 124.89 and 99.2 ($p < 0.001$), respectively (Fig. 4). The mean Phred quality score (before modification, 33.95; after modification, 31.7) were not significantly different ($p > 0.05$) and the mapping quality rate score was 60 in all cases, before and after.

3. Genetic landscape of glioblastomas

The NGS mutational analysis and Sanger sequencing detected 328 genetic alterations, including 201 non-synonymous SNVs, 36 truncating variants (stop-gain, frameshift, or splice-disrupting variant), seven in-frame indels, 82 CNAs, and two fusions (S3 Table).

Seventeen out of 25 cases (68%) harbored a *TERT* promoter mutation. Whole chromosome 7 gain was detected in 19 cases (76%), and whole chromosome 10 loss was detected in 14 cases (64%). *MGMT* promoter methylation was found in 56% of the cases. Six out of 25 cases (24%) showed *EGFR* amplification. The other genetic alterations observed are shown in Fig. 5. The landscape of glioblastomas evaluated in our study was not significantly different from those of other studies.

Discussion

As the diagnostic criteria for brain tumors have been more detailed and molecular techniques for their diagnosis have been developed, various genes related to their prognosis have come into the spotlight, such as *TERT* [10,12] or *EGFR* [21]. The detection of alterations in these genes can be used to predict a worse prognosis and to choose an appropriate

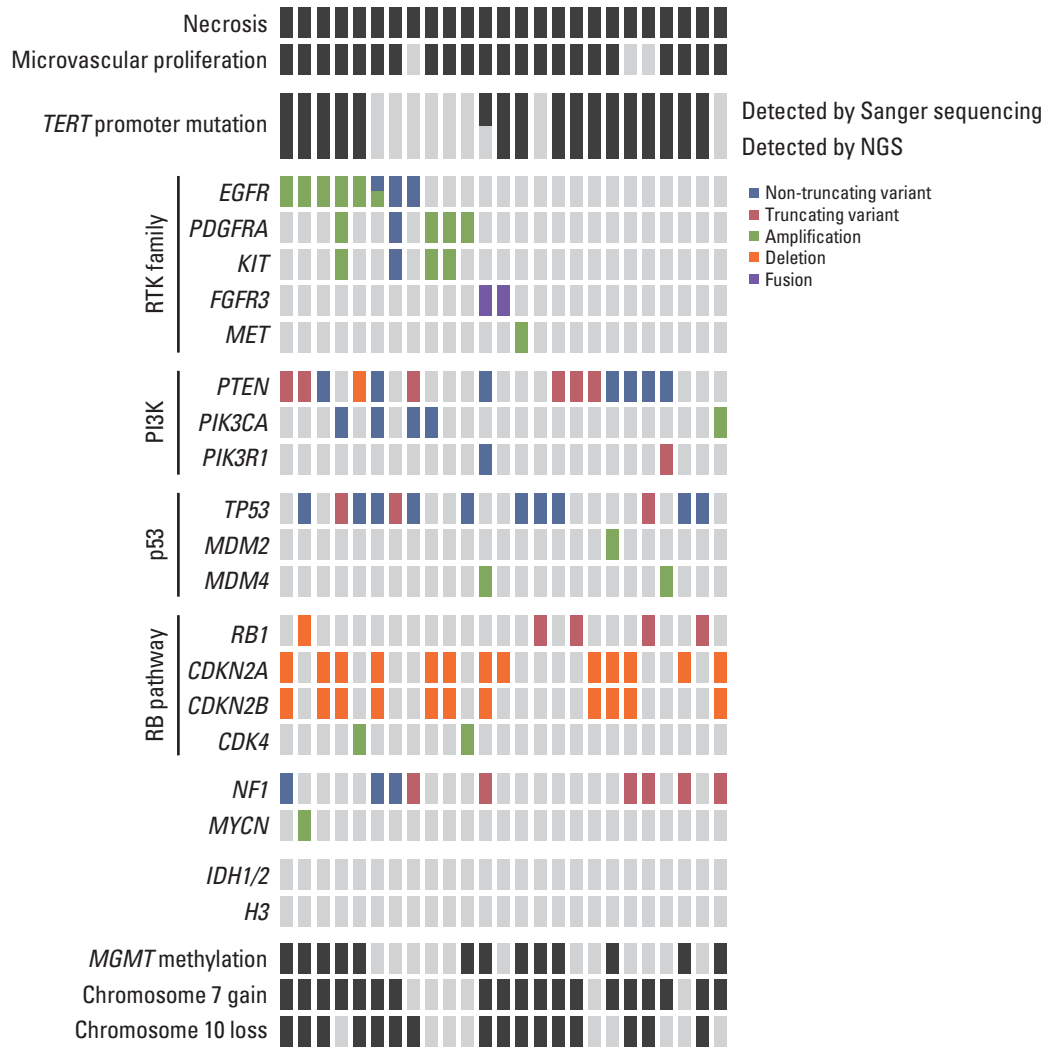


Fig. 5. Genetic and histological landscape of glioblastomas. We excluded variants which had been reported as benign or likely benign in ClinVar (<https://www.ncbi.nlm.nih.gov/clinvar/>). *CDK4*, cyclin-dependent kinase 4; *CDKN2A/B*, cyclin-dependent kinase inhibitor 2A/B; *EGFR*, epidermal growth factor receptor; *FGFR3*, fibroblast growth factor receptor 3; *IDH1/2*, isocitrate dehydrogenase 1/2; *MGMT*, O-6-methylguanine-DNA-methyltransferase; *NF1*, neurofibromin 1; NGS, next-generation sequencing; *PDGFRA*, platelet-derived growth factor receptor A; PI3K, phosphoinositide 3-kinase; RB, retinoblastoma; RTK, receptor tyrosine kinase; *TERT*, telomerase reverse transcriptase.

treatment strategy and increase the survival of patients with gliomas.

In particular, recurrent mutations in two sites of the *TERT* promoter region have been found in Chr 5:1,295,228 and Chr 5:1,295,250, which are referred to as C228T and C250T, respectively. About 72%-90% of glioblastomas [3,6] and 95% of oligodendrogliomas [21,22] show a mutation of the *TERT* promoter in these two hotspots. Among histologically proven WHO grade II or III *IDH*-wildtype diffuse astrocytic gliomas, tumors with genetic alterations (*EGFR* amplification, +7/-10, *TERT* promoter mutations) are associated with an aggressive

clinical behavior and show DNA-methylation profiles similar to those of *IDH*-wildtype glioblastomas [21,22]. In line with this, cIMPACT-NOW announced that for *IDH*-wildtype gliomas with *TERT* promoter mutations, *EGFR* amplification or whole chromosome 7 gain/10 loss was predicted to show a prognosis similar to that of glioblastomas and could be classified as a glioblastoma [8]. Therefore, the evaluation of *TERT* promoter mutations can be a critical step in the diagnosis of high-grade astrocytic tumors.

However, the *TERT* promoter region contains a GC-rich region [10] and forms a secondary structure, such as a hair-

pin structure, during PCR. It is usually amplified unsuccessfully and may show false-negative results [9]. Therefore, numerous approaches have been attempted for the appropriate amplification of genes having GC-rich regions: modification of the cycling environment, such as the temperature or cooling time [23,24]; the addition of various organic molecules, including dimethylsulfoxide [25]; or increasing the concentration of chemicals important to the amplification process, such as MgCl₂ [26].

In high-throughput sequencing, the read depth of the GC-rich region is significantly lower than that of other regions [27], and has been a chronic problem in NGS data analysis. The unimodal GC curve shows that the read depth of GC-poor or GC-rich fragments is significantly lower than the average read depth [27]. Hybrid capture-based NGS is expected to be more vulnerable to GC bias due to an unexpected behavior in the solution-hybridization process [28].

In the present study, *TERT* mutations were initially not detected using targeted NGS, but were detected using Sanger sequencing, and to explore the different detection rates of mutations in the *TERT* promoter using NGS and Sanger sequencing, we checked the filtering guidelines of our targeted NGS. We found variants, but they showed TD values lower than 50 or VCs lower than 4. These variants were removed by our filtering guidelines to exclude fake variants caused by sequencing errors. These results were similar to those of a previous study by Sahm et al. [29]. They also reported that calls from the *TERT* promoter position were filtered because the average read depth of the hotspot of the *TERT* promoter was low. The present study demonstrated that a manual review of the aligned reads using the IGV showed a *TERT* promoter mutation in 68% of the 25 cases. Therefore, given that a poor read depth due to GC bias in the GC-rich region is a problem, it is necessary to manually check the reads directly without relying on filtering. Besides a manual review of the aligned reads, there are other methods that can be used to minimize the GC bias. To compensate for the poor amplification of GC-rich sequences, we attempted to expand the target area of the *TERT* promoter region captured through baits. During the process of target capture, the baits hybridize with genomic targets of interest and select target sequences from DNA libraries for amplification. Therefore, by designing baits of the *TERT* promoter region more tightly and increasing the number of baits targeting the *TERT* promoter region, the probability of the amplification of the targeted region was increased to reach a meaningful quality for amplification.

In addition to the GC content, several factors may be associated with biases in the NGS analysis. Chen et al. [30] reported that DNA synthesis bias and PCR stochasticity bias impacted the NGS bias to a greater extent than the GC bias.

They also introduced a computational model predicting the molecular bias produced by the DNA synthesis and PCR sequencing retrieval process [30].

This study is signifying because it proposes an enforceable solution different from those presented in previous studies, such as increasing the amount of sequencing data or maintaining the 'fragment length' of DNA data [27]. It will also benefit many institutions that are preparing to design customized NGS panels for patients with brain tumors. In addition to *TERT*, the first exon of genes and the 5' untranslated region or promoter region containing GC-rich regions [31] can provide important clinical information for patients.

In conclusion, we reaffirmed the harmful influence of GC bias in the interpretation of NGS data and provided a strategy for optimizing the NGS data analysis. Although high-throughput NGS provides abundant data, the underestimation of molecular bias can lead to the obsolescence of major portions of these data. Therefore, it is crucial to keep in mind the importance of molecular bias and to carefully interpret NGS data.

Electronic Supplementary Material

Supplementary materials are available at Cancer Research and Treatment website (<https://www.e-ert.org>).

Ethical Statement

Our study was approved by the Institutional Review Board of Samsung Medical Center (IRB No. 2020-03-155). Informed written consent from patients was waived by the Institutional Review Board of Samsung Medical Center because of the retrospective study design.

Author Contributions

Conceived and designed the analysis: Lee H, Suh YL.

Collected the data: Lee H, Lee B, Kim DG, Cho YA, Kim JS, Suh YL.

Contributed data or analysis tools: Lee H, Lee B, Kim DG, Cho YA, Kim JS, Suh YL.

Performed the analysis: Lee H, Suh YL.

Wrote the paper: Lee H, Suh YL.

Conflicts of Interest

Conflict of interest relevant to this article was not reported.

References

- Harley CB, Kim NW, Prowse KR, Weinrich SL, Hirsch KS, West MD, et al. Telomerase, cell immortality, and cancer. *Cold Spring Harb Symp Quant Biol.* 1994;59:307-15.
- Vinagre J, Almeida A, Populo H, Batista R, Lyra J, Pinto V, et al. Frequency of TERT promoter mutations in human cancers. *Nat Commun.* 2013;4:2185.
- Eckel-Passow JE, Lachance DH, Molinaro AM, Walsh KM, Decker PA, Sicotte H, et al. Glioma groups based on 1p/19q, IDH, and TERT promoter mutations in tumors. *N Engl J Med.* 2015;372:2499-508.
- Horn S, Figl A, Rachakonda PS, Fischer C, Sucker A, Gast A, et al. TERT promoter mutations in familial and sporadic melanoma. *Science.* 2013;339:959-61.
- Labussiere M, Di Stefano AL, Gleize V, Boisselier B, Giry M, Mangesius S, et al. TERT promoter mutations in gliomas, genetic associations and clinico-pathological correlations. *Br J Cancer.* 2014;111:2024-32.
- Killela PJ, Reitman ZJ, Jiao Y, Bettegowda C, Agrawal N, Diaz LA Jr, et al. TERT promoter mutations occur frequently in gliomas and a subset of tumors derived from cells with low rates of self-renewal. *Proc Natl Acad Sci U S A.* 2013;110:6021-6.
- Louis DN, Perry A, Reifenberger G, von Deimling A, Figarella-Branger D, Cavenee WK, et al. The 2016 World Health Organization classification of tumors of the central nervous system: a summary. *Acta Neuropathol.* 2016;131:803-20.
- Brat DJ, Aldape K, Colman H, Holland EC, Louis DN, Jenkins RB, et al. cIMPACT-NOW update 3: recommended diagnostic criteria for "Diffuse astrocytic glioma, IDH-wildtype, with molecular features of glioblastoma, WHO grade IV". *Acta Neuropathol.* 2018;136:805-10.
- Mitas M, Yu A, Dill J, Kamp TJ, Chambers EJ, Haworth IS. Hairpin properties of single-stranded DNA containing a GC-rich triplet repeat: (CTG)₁₅. *Nucleic Acids Res.* 1995;23:1050-9.
- Colebatch AJ, Witkowski T, Waring PM, McArthur GA, Wong SQ, Dobrovic A. Optimizing amplification of the GC-rich TERT promoter region using 7-deaza-dGTP for droplet digital PCR quantification of TERT promoter mutations. *Clin Chem.* 2018;64:745-7.
- Diplas BH, Liu H, Yang R, Hansen LJ, Zachem AL, Zhao F, et al. Sensitive and rapid detection of TERT promoter and IDH mutations in diffuse gliomas. *Neuro Oncol.* 2019;21:440-50.
- Li H, Durbin R. Fast and accurate long-read alignment with Burrows-Wheeler transform. *Bioinformatics.* 2010;26:589-95.
- Li H. A statistical framework for SNP calling, mutation discovery, association mapping and population genetical parameter estimation from sequencing data. *Bioinformatics.* 2011;27:2987-93.
- McKenna A, Hanna M, Banks E, Sivachenko A, Cibulskis K, Kernytzky A, et al. The Genome Analysis Toolkit: a MapReduce framework for analyzing next-generation DNA sequencing data. *Genome Res.* 2010;20:1297-303.
- Cibulskis K, Lawrence MS, Carter SL, Sivachenko A, Jaffe D, Sougnez C, et al. Sensitive detection of somatic point mutations in impure and heterogeneous cancer samples. *Nat Biotechnol.* 2013;31:213-9.
- Wilm A, Aw PP, Bertrand D, Yeo GH, Ong SH, Wong CH, et al. LoFreq: a sequence-quality aware, ultra-sensitive variant caller for uncovering cell-population heterogeneity from high-throughput sequencing datasets. *Nucleic Acids Res.* 2012;40:11189-201.
- Lai Z, Markovets A, Ahdesmaki M, Chapman B, Hofmann O, McEwen R, et al. VarDict: a novel and versatile variant caller for next-generation sequencing in cancer research. *Nucleic Acids Res.* 2016;44:e108.
- Shin HT, Choi YL, Yun JW, Kim NK, Kim SY, Jeon HJ, et al. Prevalence and detection of low-allele-fraction variants in clinical cancer samples. *Nat Commun.* 2017;8:1377.
- Ye K, Schulz MH, Long Q, Apweiler R, Ning Z. Pindel: a pattern growth approach to detect break points of large deletions and medium sized insertions from paired-end short reads. *Bioinformatics.* 2009;25:2865-71.
- Kim H, Kwon MJ, Park B, Choi HG, Nam ES, Cho SJ, et al. Negative prognostic implication of TERT promoter mutations in human papillomavirus-negative tonsillar squamous cell carcinoma under the new 8th AJCC staging system. *Indian J Surg Oncol.* 2020;12:134-43.
- Suzuki H, Aoki K, Chiba K, Sato Y, Shiozawa Y, Shiraishi Y, et al. Mutational landscape and clonal architecture in grade II and III gliomas. *Nat Genet.* 2015;47:458-68.
- Cancer Genome Atlas Network; Brat DJ, Verhaak RG, Aldape KD, Yung WK, Salama SR, et al. Comprehensive, integrative genomic analysis of diffuse lower-grade gliomas. *N Engl J Med.* 2015;372:2481-98.
- Hube F, Reverdiau P, Iochmann S, Gruel Y. Improved PCR method for amplification of GC-rich DNA sequences. *Mol Biotechnol.* 2005;31:81-4.
- Frey UH, Bachmann HS, Peters J, Siffert W. PCR-amplification of GC-rich regions: 'slowdown PCR'. *Nat Protoc.* 2008;3:1312-7.
- Chakrabarti R, Schutt CE. The enhancement of PCR amplification by low molecular weight amides. *Nucleic Acids Res.* 2001;29:2377-81.
- Kramer MF, Coen DM. Enzymatic amplification of DNA by PCR: standard procedures and optimization. *Curr Protoc Immunol.* 2001;Chapter 10:Unit 10.20.
- Benjamini Y, Speed TP. Summarizing and correcting the GC content bias in high-throughput sequencing. *Nucleic Acids Res.* 2012;40:e72.
- Mertes F, Elsharawy A, Sauer S, van Helvoort JM, van der Zaag PJ, Franke A, et al. Targeted enrichment of genomic DNA regions for next-generation sequencing. *Brief Funct Genomics.* 2011;10:374-86.
- Sahm F, Schrimpf D, Jones DT, Meyer J, Kratz A, Reuss D, et al. Next-generation sequencing in routine brain tumor diagnostics enables an integrated diagnosis and identifies actionable targets. *Acta Neuropathol.* 2016;131:903-10.
- Chen YJ, Takahashi CN, Organick L, Bee C, Ang SD, Weiss P, et al. Quantifying molecular bias in DNA data storage. *Nat Commun.* 2020;11:3264.
- Antequera F, Bird A. Number of CpG islands and genes in human and mouse. *Proc Natl Acad Sci U S A.* 1993;90:11995-9.